Noise Transfer Function Design and Optimization for Digital Sigma-Delta Audio DAC

Marcin LEWANDOWSKI

Warsaw University of Technology
Institute of Radioelectronics
Nowowiejska 15/19, 00-665 Warszawa, Poland
e-mail: M.Lewandowski@ire.pw.edu.pl

The parameters of sigma-delta audio DAC depend mainly on digital sigma-delta modulator's features, especially on its noise transfer function (NTF). Many methods of design and optimization of the loop filter's coefficients in sigma-delta modulators have been proposed so far. These methods enable the designer to get suitable noise transfer functions for specific application. This paper reviews NTF design and optimization methods which are particularly useful in audio applications.

Keywords: noise transfer function (NTF), NTF design, NTF optimization, sigma-delta modulation, sigma-delta audio DAC, psychoacoustic NTF optimization, NTF stability criteria.

1. Introduction

Recently, sigma-delta DACs (oversampled noise-shaping DACs) have become an attractive alternative to conventional R-2R DACs (Nyquist rate PCM or oversampled PCM) (KULKA, 2006). Generally, they offer higher integration at lower cost, a possibility of implementation in modern sub micron CMOS VLSI technologies with on-chip digital interpolation filters as well as with additional digital signal processing functions, relatively easy implementation in FPGA structures (KULKA, WOSZCZEK, 2008, cited by KULKA, LEWANDOWSKI, 2009), higher resolution without additional component trimming or calibration, single voltage power supply (typ. 5 V) and lower power dissipation. These advantages, compared to conventional R-2R DACs, significantly reduce manufacturing costs. Sigma-delta DACs are now widely used both in consumer and professional digital audio systems.

A typical sigma-delta DAC, shown in Fig. 1, consists of a digital interpolation filter (DIF), a lowpass digital sigma-delta modulator (DSDM), an internal 1- or

K-bit DAC and an analog lowpass post-DAC filter (ALPF). The DIF performs an upsampling operation of a multibit digital input signal. That is, a stream of B-bit words with a sampling rate of fs changes to a stream of B'-bit words (usually, $B' > B$) with a sampling rate of $L \cdot fs$, where L is the oversampling ratio. The DSDM shortens the word length to a single bit or to K bits (usually, $K \ll B'$) and spectrally shapes the truncation (requantization) noise which can be viewed as pushing noise power from the signal band to higher frequencies. The truncated output signal of the DSDM (i.e. a 1- or K-bit data stream with a rate of $L \cdot fs$) is converted to an analog signal by the internal DAC. Finally, the analog output of the internal DAC is fed to the ALPF for out-of-band noise filtering and analog signal reconstruction (KULKA, LEWANDOWSKI, 2009).
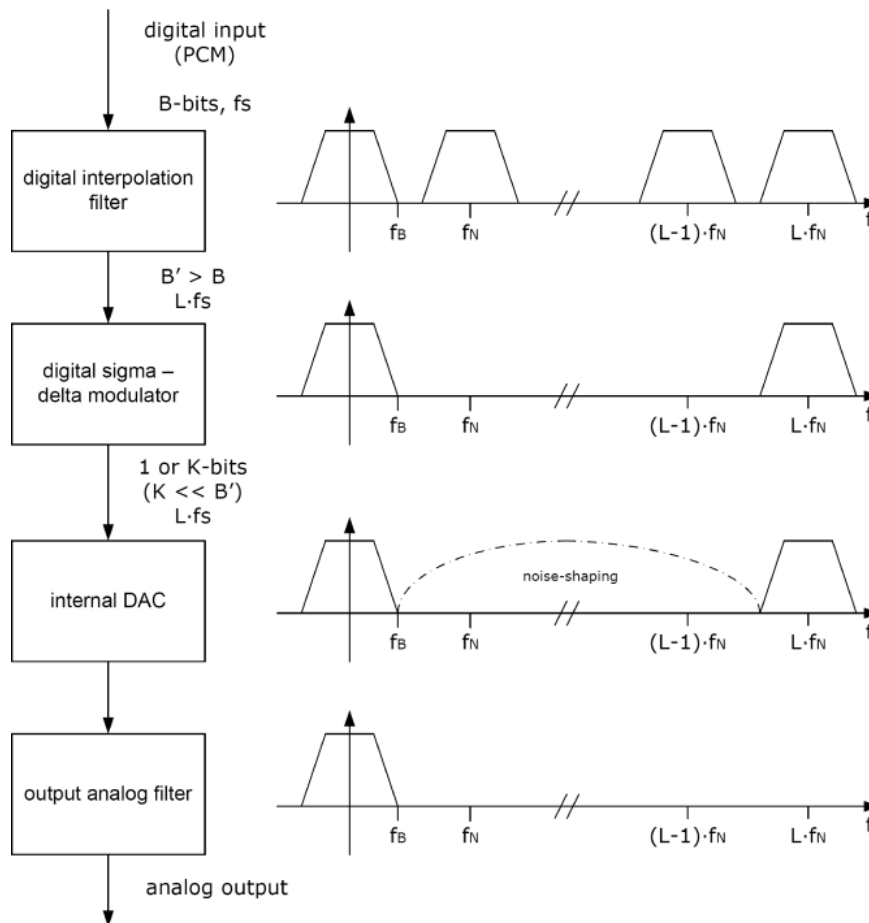

Fig. 1. Block diagram of a typical sigma-delta DAC.

The most important audio DACs (also ADCs) specifications are: signal to noise ratio (SNR), dynamic range (DR) and total harmonic distortion plus noise

(THD+N). Depending on application sigma-delta DACs can have the following parameters: 90–120 dB SNR/DR and 90–110 dB THD+N. The digital loop filter and its noise transfer function (NTF) play the most crucial role in order to obtain required parameters of the high oversampled sigma-delta DAC (KULKA, LEWANDOWSKI, 2009).

This paper presents chosen methods of designing and optimization of the loop filter's coefficients in sigma-delta modulators, which allow the designer to get suitable noise transfer functions. Furthermore, the NTF design and optimization methods, which are particularly useful in audio applications are presented.

2. Truncation noise shaping

The main task of the DSDM is shaping the noise in such a way that a high portion of the noise energy is contained above the audio signal bandwidth. This is done by the DSDM's loop filter, which is shown in Fig. 2 (KULKA, WOSZCZEK, 2008).
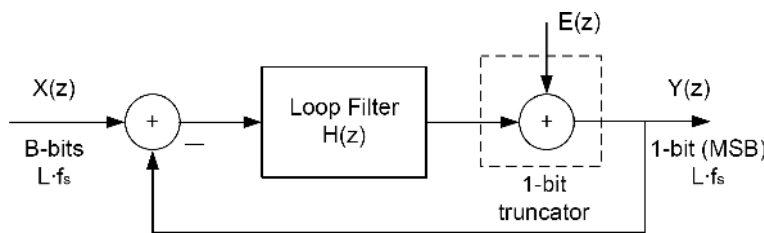

Fig. 2. The linear model of single-loop 1-bit DSDM with MSB feedback.

The DSDM's output signal $Y(z)$ is a superposition of the input signal $X(z)$ and the truncation noise signal $E(z)$ (modeled as an additive, white noise). The output signal $Y(z)$ is transformed according to the formula (LØKKEN, 2005):

$$Y(z) = X(z) \cdot z^{-1} + E(z) \cdot (1 - z^{-1}). \tag{1}$$

By following the signal flow in Fig. 2, the transfer function from input to output (STF – signal transfer function) and from the truncator to output (NTF – noise transfer function) can be derived as follows (LØKKEN, 2005):

$$\text{STF}(z) = z^{-1}, \tag{2}$$

$$\text{NTF}(z) = 1 - z^{-1}. \tag{3}$$

Thus, the input signal $X(z)$ has been delayed by just one sample, while the truncation noise signal $E(z)$ has been passed through a high-pass filter. This is shown in Fig. 3. The combination of noise shaping in the DSDM's loop filter with an oversampling (which is shown in Fig. 3) significantly improves the SNR value.
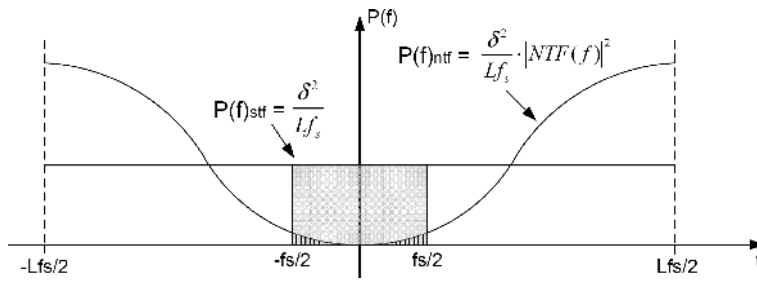
Fig. 3. Oversampling and noise shaping in sigma-delta modulator.

The SNR value for large oversampling ratios (L) with B-bit representation can be approximated by (LØKKEN, 2005):

$$\text{SNR [dB]} \approx 6.02 \cdot B + 1.76 - 10 \cdot \log\left(\frac{\pi^{2N}}{2N+1}\right) + 10 \cdot \log(2N+1) \cdot \log(L). \quad (4)$$

The SNR gain vs. the oversampling ratio L based on Eq. (4) was simulated in Matlab and is given in Fig. 4. Seemingly, to achieve very high value of the SNR, the high order DSDM and the high oversampling ratio can be used. Unfortunately, the $(1-z^{-1})^N$-modulators are highly prone to instability and thus different NTFs
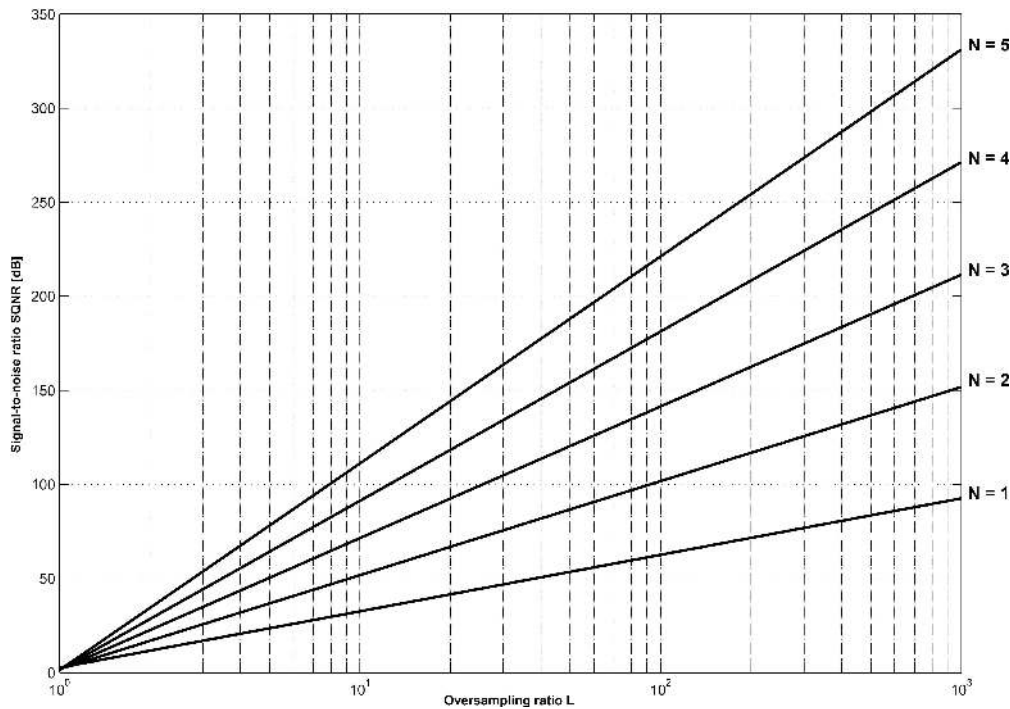

Fig. 4. Signal-to-noise ratio vs. oversampling ratio L with DSDM order N as parameter for $(1-z^{-1})^N$-modulators.

must be used. Design of stable and high-performing modulators is one of the most challenging and crucial matter in sigma-delta DACs design.

3. NTF selection criteria

The design of a sigma-delta modulator requires the selection of appropriate NTF so that the modulator would be stable and at the same time could achieve high SNR. For this purpose, the NTF should posses the following characteristics (BOURDOPOULOS *et al.*, 2003):

- The truncation noise has to be delayed by at least one sampling period before returning to the truncator input. Thus, the first term of the impulse response of the NTF should always be equal to 1 (NORSWORTHY *et al.*, 1997). In this case, sigma-delta modulator is a causal system.
- The NTF is of the form, where g is a constant (BOURDOPOULOS *et al.*, 2003):

$$\text{NTF}(z^{-1}) = g \cdot \prod_{i=1}^{n} \frac{\left(1 - z_i \cdot z^{-1}\right)}{\left(1 - p_i \cdot z^{-1}\right)}, \tag{5}$$

where z_i are zeros and p_i are poles. Using Taylor series expansion around $z^{-1} = 0$, for the first term of the impulse response (h_0) it will be:

$$h_0 = \text{NTF}(0) = g. \tag{6}$$

Consequently, $g = 1$ and this has to be taken into consideration when an ordinary transfer function is to be selected from tabulated data.

- The sigma-delta modulator's output sequence has always constant power δ^2, which is composed of the signal power (P_x) and the total noise power ($P_{e-\text{tot}}$) (BOURDOPOULOS *et al.*, 2003):

$$P_x + P_{e-\text{tot}} = \delta^2. \tag{7}$$

The signal power (P_x), which can be properly processed by the sigma-delta modulator, decreases as the noise power (P_e) increases. If the truncation noise spectrum is white, then:

$$P_{e-\text{tot}} = \frac{P_e}{2\pi} \int_{-\pi}^{\pi} \left| \text{NTF}(e^{j\theta}) \right|^2 \, \mathrm{d}\theta = P_e \cdot A, \tag{8}$$

where θ is a frequency in radians, A is the noise amplification factor and P_e is white noise power.

- The truncation noise power within the signal band ($P_{e-\text{in}}$) depends on the order of the NTF. It is shown in (BOURDOPOULOS *et al.*, 2002) that the noise power $P_{e-\text{in}}$ is given approximately by (BOURDOPOULOS *et al.*, 2003):

$$P_{e-\text{in}} \cong \frac{P_e}{R} \cdot \frac{1}{e} \cdot A^{-(N-1)}. \tag{9}$$

Clearly $P_{e-\text{in}}$ decreases rapidly with increasing A.

- The maximum achievable SNR is given by (BOURDOPOULOS *et al.*, 2003):

$$\text{SNR}_{\max} = \frac{P_x}{P_{e-\text{in}}} = e \cdot \frac{N}{P_e} \cdot A^{(N-1)} \cdot \left(\delta^2 - P_e \cdot A\right). \qquad (10)$$

According to Eq. (10) the maximum SNR is achieved for a high value of A and consequently, for a high order NTF. However, this results in increasing the $P_{e-\text{tot}}$ and, according to Eq. (7), decreasing the tolerable P_x. Therefore, for encoding high values of the input signal, a compromise leading to lower SNR must be accepted.

- The NTF with minimum phase will lead to higher SNR. Otherwise, a constant g in Eq. (5) will be greater than 1, which will result in an increase in the truncation noise power $P_{e-\text{in}}$ and decrease in the SNR (BOURDOPOULOS *et al.*, 2003).

3.1. Stability criteria

Various stability criteria for selecting the appropriate NTF and thus assessing the functionality of a digital sigma-delta modulator can be found in literature. Most of them are based on extensive simulations. The chosen ones are the following:

- The sum of the absolute value of terms in the impulse response of the NTF $(S_{|h|})$ is bounded (ANASTASSIOU, 1989, cited by SCHREIER, 1993):

$$S_{|h|} \equiv \sum_{i=0}^{\infty} |h_i| = 3 - x_{\max}, \qquad (11)$$

where $x_{\max}$ is the maximum signal amplitude for which the modulator remains stable. In practice, the criterion is usually applied in the form $S_{|h|} < c$, where $c \approx 3.5$.

- The mean-squared value of the magnitude response of the NTF(A) has to be smaller than 2.5 (ANASTASSIOU, 1989, cited by SCHREIER, 1993):

$$A \equiv \frac{1}{2\pi} \int_{-\pi}^{\pi} \left|\text{NTF}(e^{j\theta})\right|^2 \, \mathrm{d}\theta < 2.5. \qquad (12)$$

- The maximum value of the frequency response of the NTF(M) has to be smaller than 2 (SCHREIER, 1993; CHAO *et al.*, 1990):

$$M \equiv \max\left\{|\text{NTF}(z)|\right\} < 2. \qquad (13)$$

- The value of S_{h^2} (sum of squared impulse response values) after extensive simulations is found to be (BOURDOPOULOS, 1999, cited by BOURDOPOULOS *et al.*, 2002):

$$S_{h^2} \equiv \sum_{i=2}^{\infty} h_i^2 < 0.07. \qquad (14)$$

- For modulator orders from 3 to 8 the noise amplification factor (A) is bounded (Kuo *et al.*, 1999):

$$A \leq A_{\max} = C - 3P_{x\,\max}, \tag{15}$$

$$A \geq A_{\min} = 1.5 - 0.04 \cdot (N - 3), \tag{16}$$

where constant C was found after simulations (depending on N), and stability regions are shown in Fig. 5.
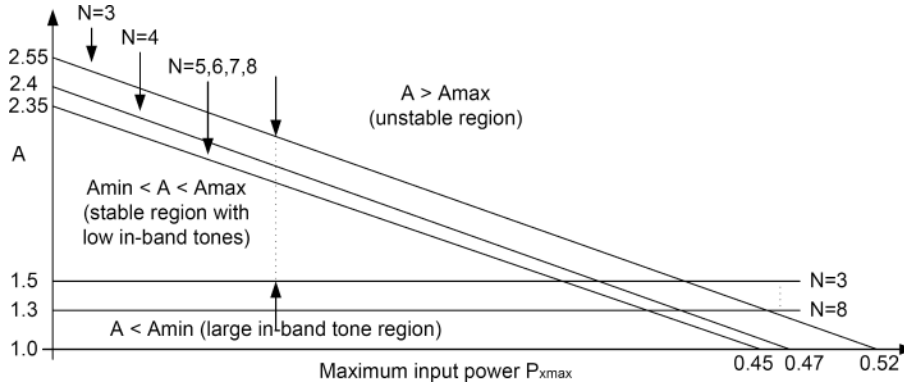

Fig. 5. Acceptable NTF regions for orders from $N = 3$ to $N = 8$ (Kuo *et al.*, 1999).

4. Noise transfer function determination

The noise transfer function (NTF) design process can be divided into several basic steps (Norsworthy *et al.*, 1997):
- choosing a modulator order and the NTF filter family,
- putting up a value for the filter cutoff frequency and scale the transfer function so that the first sample of the impulse response is 1,
- constructing a modulator with this NTF and either simulate it (e.g. in Matlab Simulink) or use the describing function method to determine its maximum stable input and peak SNR,
- determining (taking into account the content of Subsec. 3.1) the NTF as a compromise between the maximum level of the input signal and the maximum value of the SNR in order to stabilize the modulator's operation.

4.1. Filter selection for NTF designing

Three filter families are taken into consideration in designing the NTF:
- Pure N-th order differentiators (Norsworthy *et al.*, 1997):

$$H(z) = (1 - z^{-1})^N. \tag{17}$$

These functions meet the causality requirement, established in Sec. 3, that the first value of the impulse response must be equal to 1. The magnitude response

of $H(z)$ for various values of N was simulated using $expand(\ )$ function in Matlab and is shown in Fig. 6. Note that at high values of N, more effective suppression of the truncation noise can be obtained at low frequencies but there is more gain at high frequencies, which can lead (according to Eqs. (11) and (12)) to the instability of the modulator (NORSWORTHY $et\ al.$, 1997).
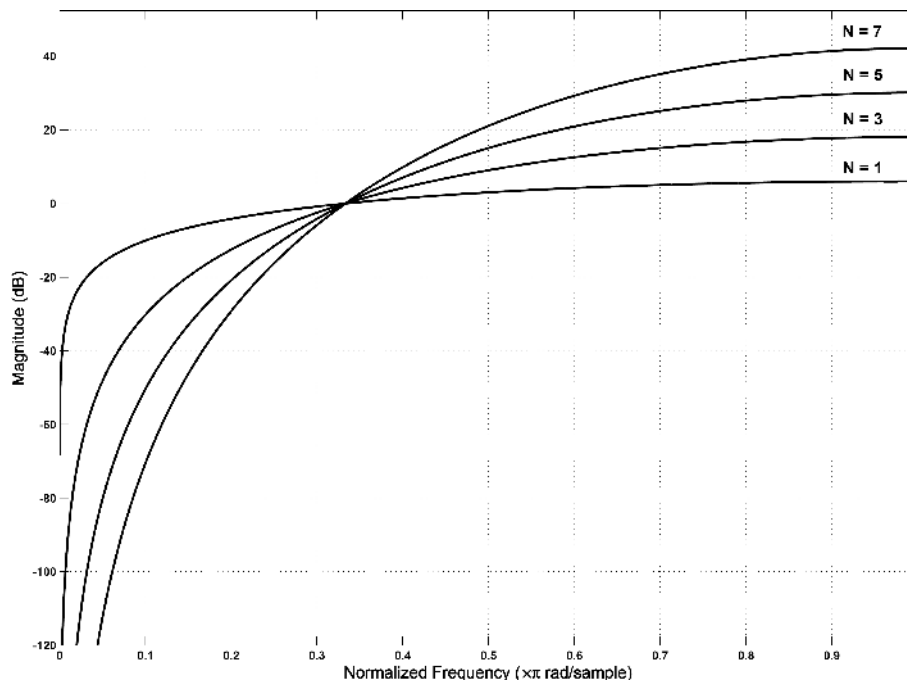

Fig. 6. Pure differentiator NTFs for orders $N = 1, 3, 5$ and 7.

- The problem encountered in the previous noise-shaping function was the large high-frequency noise-shaping gain for large N. In order to flatten the high-frequency portion of $H(z)$ poles are introduced into the pure differentiating response. With a $Butterworth$ alignment of the poles, which was simulated using $butter(\ )$ function in Matlab, a maximally flat high-frequency region of $H(z)$ can be obtained as shown in Fig. 7 (NORSWORTHY $et\ al.$, 1997).
- The $Butterworth$ high-pass response can be modified to move the real stopband zeros at the $(1, \mathrm{j}0)$-dc point out on the unit circle to produce nulls in the NTF at frequencies other than dc. Compared to the $Butterworth$, with the $Inverse\text{-}Chebyshev$ alignment, improved signal-to-noise ratio can be obtained (NORSWORTHY $et\ al.$, 1997). An example of the 5th order $Inverse\text{-}Chebyshev$ noise transfer function's zeros and poles placement is shown in Fig. 8 and the noise transfer function characteristic is shown in Fig. 9. Both figures were obtained using functions $cheby2(\ )$ and $fvtool(\ )$ in Matlab.
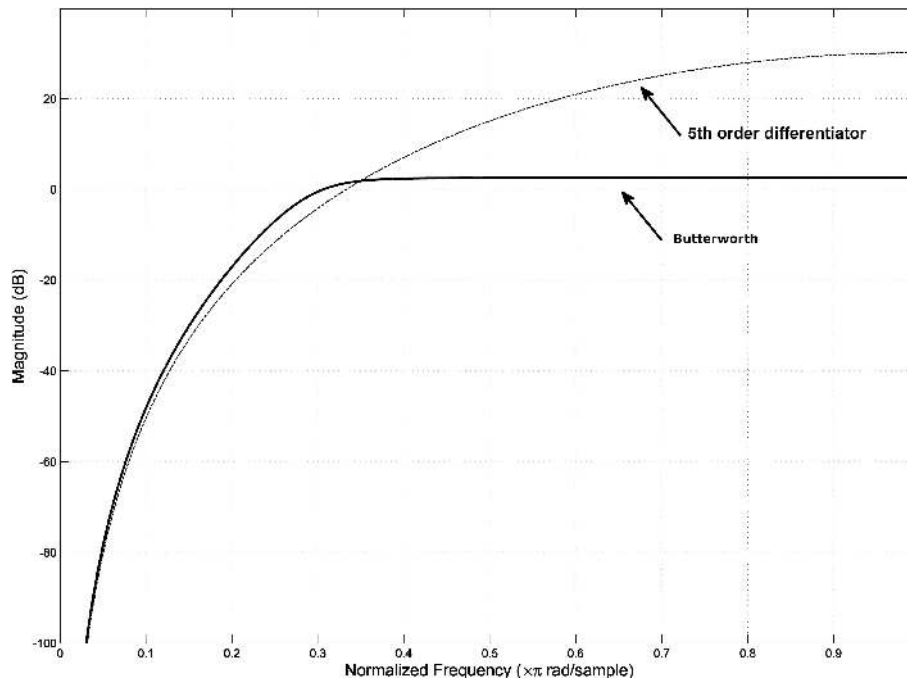
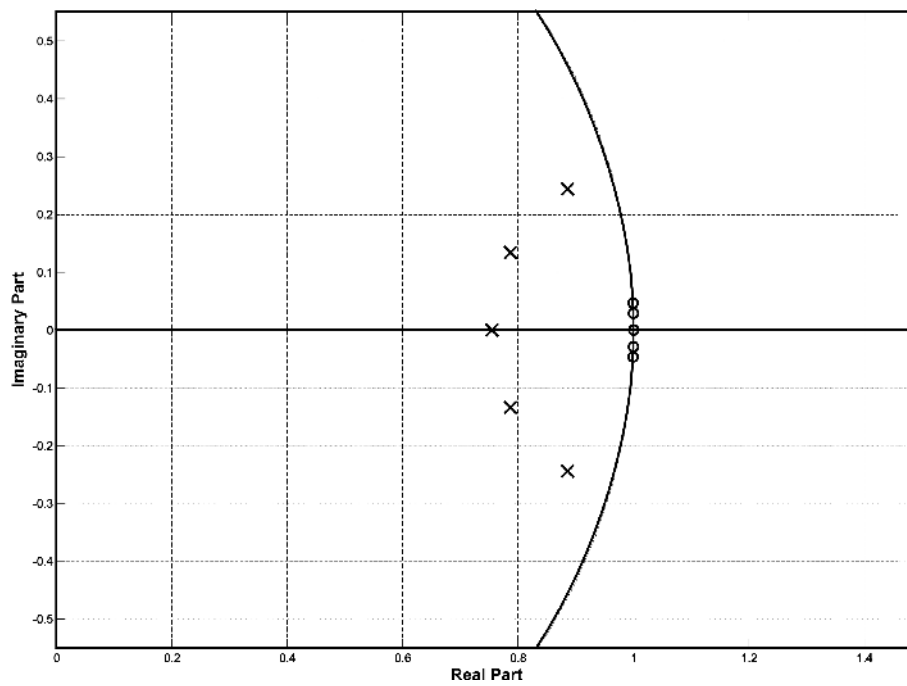Fig. 7. *Butterworth* NTF characteristic compared to 5th order differentiator.

Fig. 8. *Inverse-Chebyshev* NTF's zeros and poles placement for $N = 5$ order.
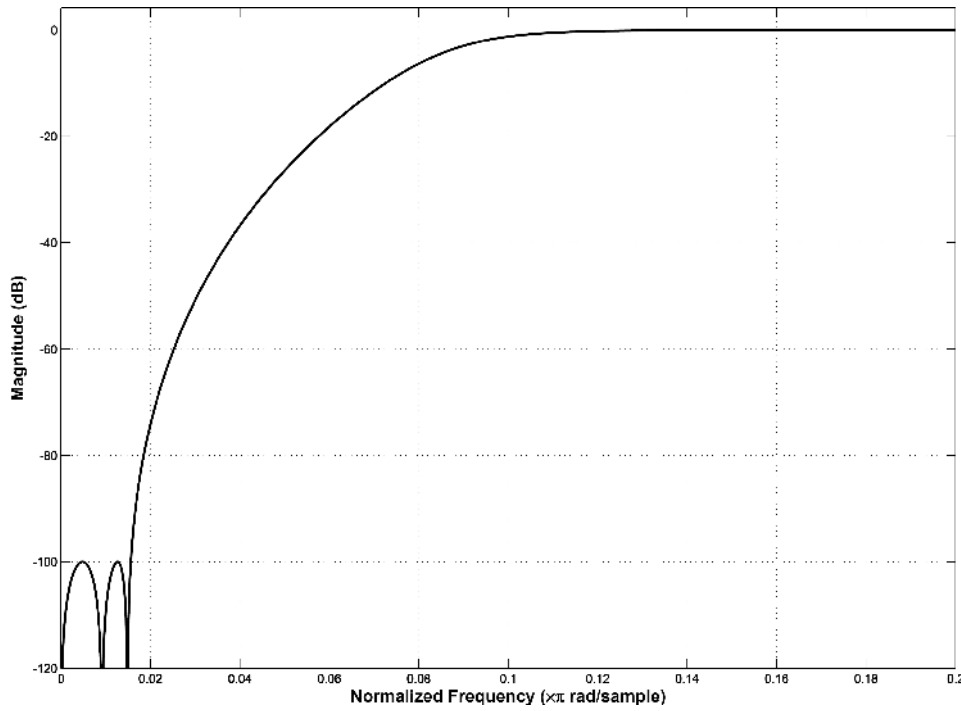
Fig. 9. 5th order *Inverse-Chebyshev* NTF characteristic.

5. NTF optimization

All mentioned in Sec. 4 NTF design methods are the basis for subsequent optimization the zeros' and poles' position of the NTF. The purpose of optimizing the zeros' location within the unit circle is to reduce the noise power in the signal band, while optimizing the position of poles reduces the out-of-band NTF gain, resulting in improved stability of a modulator. Determining an optimal NTF is related to finding first the best position of zeros and then the position of poles.

5.1. Optimizing the position of zeros

The position of zeros should be such that the power of the truncation noise in the signal band is minimized (SCHREIER, 1993). This means that the following integral should be minimized (BOURDOPOULOS *et al.*, 2003):

$$C_1 = \int\limits_0^{\pi/L} \left| \mathrm{NUM}(e^{j\theta}) \right|^2 \, \mathrm{d}\theta. \tag{18}$$

Since zeros lie on the unit circle, they can be written in the form of $e^{j\phi_i}$. Then, since $\theta, \phi_i \leq \pi/L \ll 1$, for $z = e^{j\theta}$ and for even N (BOURDOPOULOS *et al.*, 2003):

$$\text{NUM}(z^{-1}) = \prod_{i=1}^{N/2} \left(1 - e^{-j(\phi_i+\theta)}\right)\left(1 - e^{j(\phi_i-\theta)}\right)$$

$$\approx \prod_{i=1}^{N/2} \left(\phi_i^2 - \theta^2\right) = \sum_{i=0}^{N/2} b_i \theta^{2i} \qquad (19)_1$$

while for odd N (BOURDOPOULOS *et al.*, 2003):

$$\text{NUM}(z^{-1}) = \left(1 - e^{-j\theta}\right) \prod_{i=1}^{(N-1)/2} \left(1 - e^{-j(\phi_i+\theta)}\right)\left(1 - e^{j(\phi_i-\theta)}\right)$$

$$\approx j\theta \sum_{i=0}^{(N-1)/2} b_i \theta^{2i}. \qquad (19)_2$$

In order to evaluate the coefficients b_i, expressions for $\text{NUM}(z^{-1})$ from Eq. $(19)_1$ and Eq. $(19)_2$ are inserted into Eq. (18). Evaluation of integral (frequency π/L was normalized to 1) leads to the following set (BOURDOPOULOS *et al.*, 2003):

$$\sum_{i=0}^{N/2-1} \frac{b_i}{2k + 2i + 1} = -\frac{(-1)^{N/2}}{N + 2k + 1}, \qquad k = 0, 1, \ldots, \frac{N}{2} - 1 \qquad (20)_1$$

for even N and:

$$\sum_{i=0}^{(N-1)/2-1} \frac{b_i}{2k + 2i + 3} = -\frac{(-1)^{(N-1)/2}}{N + 2k + 2}, \qquad k = 0, 1, \ldots, \frac{N-1}{2} - 1 \qquad (20)_2$$

for odd N and coefficient $b_{N/2} = (-1)^{N/2}$. The roots of the polynomials $(19)_1$ and $(19)_2$ are referred to as optimal. In Table 1 the performance achieved by the optimal and *Inverse-Chebyshev* polynomials, when compared to the ω^N polynomials, which have all their roots at zero, is presented (BOURDOPOULOS *et al.*, 2003).

Table 1. SNR improvement compared to *dc* zero set (BOURDOPOULOS *et al.*, 2003).

Order N	SNR improvement [dB]	
	Optimal	Inverse-Chebyshev
2	3.5	2.3
3	7.9	6.7
4	12.8	11.6
5	17.9	16.7

Another method for optimizing the position of zeros was proposed in (SCHREIER, 1993). Schreier derived the following analytical expression which approximately relates the in-band (unweighted) noise power N_u^2 to zero frequencies f_i by:

$$N_u^2 = k \int\limits_0^{f_B} \prod_{i=1}^{N} (f - f_i)^2 \, \mathrm{d}f, \qquad (21)$$

where k is a constant and f_B is the upper signal band frequency. The resulting values for zeros (normalized to the signal band limit) are given, for NTFs orders from 1 to 8 and $f_B = 22.05$ [kHz], in Table 2.

Table 2. Optimal NTF zero locations and SNR improvement compared to *dc* zeros (DUNN, SANDLER, 1995).

Order N	f_i for $f_B = 22.05$ kHz	$\Delta\mathrm{SNR}_{dc}$
1	0	0.0
2	± 12.7	3.5
3	$0, \pm 17.1$	8.0
4	$\pm 7.5, \pm 19.0$	12.8
5	$0, \pm 11.8, \pm 20.0$	17.9
6	$\pm 5.3, \pm 14.6, \pm 20.6$	23.2
7	$0, \pm 8.9, \pm 16.4, \pm 20.9$	28.6
8	$\pm 4.0, \pm 11.6, \pm 17.6, \pm 21.2$	34.0

5.2. Optimizing the position of poles

As mentioned earlier, optimizing the position of poles reduces the out-of-band NTF gain, resulting in improved stability of a modulator. For *Inverse-Chebyshev* NTFs the position of poles can be uniquely determined by the value of the parameter A (noise amplification factor) or M (the maximum value of the NTF's impulse response), in case the latter should be constrained (Eqs. (12) and (13)). Another way for selecting the optimum position of poles was proposed by Bourdopoulos and his colleagues in their studies (BOURDOPOULOS, 1999, cited by BOURDOPOULOS *et al.*, 2002). The method relies on searching the whole region inside the unit circle to find the position of poles leading to the maximum SNR. For this purpose, the stability criterion is constrained (Eq. (14)) and the whole region is examined for poles to minimize the integral (BOURDOPOULOS *et al.*, 2003):

$$P_{e-\mathrm{in}} = \frac{P_e}{\pi} \int\limits_0^{\pi/L} \left| \mathrm{NTF}(e^{j\theta}) \right|^2 \mathrm{d}\theta. \qquad (22)$$

In Table 3 poles of the NTF are given as obtained from above presented approach.

Table 3. SNR$_{\max}$ and $X_{\max}$ comparison for *Inverse-Chebyshev* NTF and optimal NTF (BOURDOPOULOS *et al.*, 2003).

Order N	Inverse-Chebyshev		Optimized NTF	
	SNR$_{\max}$ [dB]	$X_{\max}$ [FS]	SNR$_{\max}$ [dB]	$X_{\max}$ [FS]
3	90.4	0.741	93.4	0.589
4	105.8	0.575	107.9	0.562
5	118.4	0.501	121.5	0.575

Another method for optimizing the position of poles was proposed in (SCHREIER, TEMES, 2005). The main criterion was the NTF poles, which yield a maximally-flat all-pole transfer function (SCHREIER, TEMES, 2005):

$$\left| \text{DEN}(e^{j\theta}) \right|^2 = \text{DEN}(e^{j\theta}) \cdot \left[\text{DEN}(e^{i\theta}) \right]^* = \text{DEN}(z) \cdot \text{DEN}(1/z)\,|_{z=e^{j\theta}} . \quad (23)$$

Requirement that $\left| \text{DEN}(e^{j\theta}) \right|$ should be maximally flat around $\theta = 0$ is equivalent to the condition that $\text{DEN}(z) \cdot \text{DEN}(1/z)$ should be maximally flat around $z = 1$ (SCHREIER, TEMES, 2005):

$$\text{DEN}(z) \cdot \text{DEN}(1/z) = \text{DEN}(1) + a(z-1)^N \cdot \left(\frac{1}{z} - 1 \right)^N , \quad (24)$$

where a is assumed to be some constant, which controls the sharpness of the filter characteristic. After some calculations, poles of the sought-after NTF are given by the roots of N complex quadratic equations (SCHREIER, TEMES, 2005):

$$z^2 + b_k z + 1 = 0, \qquad k = 0, 1, \ldots, N-1, \quad (25)$$

where

$$b_k = \frac{e^{j(2k+1)\pi/N}}{a^{1/N}}. \quad (26)$$

5.3. Psychoacoustically optimal NTF

In sigma-delta modulators used in audio applications, psychoacoustic considerations dictate the characteristics required of an optimal modulator. First, the noise floor due to the truncation should posses a power spectral density within the audio band that is invariant with changes in the input signal. Second, the noise floor should be minimally audible (DUNN, 1994). In the later study by Dunn and his colleague (DUNN, SANDLER, 1995) authors have presented the NTF designing method based on isophonic curves, which method was earlier specified and used in conventional PCM audio converters (LIPSHITZ *et al.*, 1991 cited by WANNAMAKER, 1992).

In the psychoacoustically optimal NTF, noise shaping poles have negligible influence in the audio band and thus, they are not taken into consideration. In order to make an SNR measurement more psychoacoustically relevant, according to Eq. (21), it is possible to accommodate this nonuniform sensitivity by

skewing the noise floor with a weighting function $W(f)$, which yields (DUNN, SANDLER, 1995):

$$N_w^2 \approx k \int_0^{f_B} W(f) \prod_{i=1}^{N} (f - f_i)^2 \, \mathrm{d}f. \tag{27}$$

The weighting function $W(f)$ was chosen to be the F-weighting function derived by WANNAMAKER (1992). The F-weighting curve in Fig. 10 is obtained by modeling the ISO 15-phon equal-loudness data for noise, with a free-to-diffuse-field correction applied. In Table 4 the performance achieved by the psychoacoustically optimal sets of zeros' location, when compared to dc zero sets, is
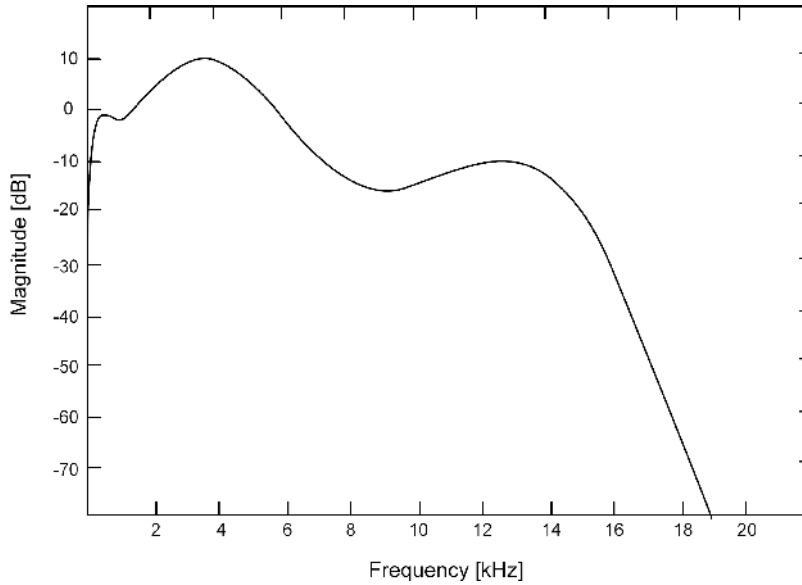

Fig. 10. F-weighting curve (WANNAMAKER, 1992).

Table 4. Weighted SNR advantages of psychoacoustically optimal zero locations relative to dc zero sets (DUNN, SANDLER, 1995).

Order N	f_i for $f_B = 22.05$ kHz	$\Delta\mathrm{SNR}_{dc}$
1	0	0.0
2	±4.014	2.1
3	0, ±6.443	2.0
4	±3.590, ±11.954	9.2
5	0, ±4.308, 12.959	14.2
6	±3.325, ±7.078, ±13.389	17.9
7	0, ±4.017, ±10.471, ±13.842	22.3
8	±2.933, ±5.167, ±12.012, ±14.381	28.0

presented. An example of the *F*-weighted 4th order NTF for psychoacoustically
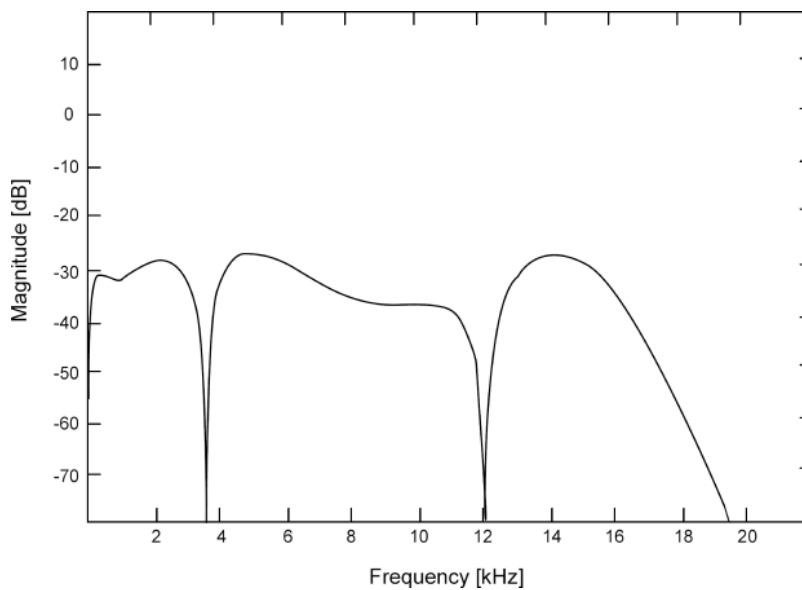optimal zero sets is shown in Fig. 11.

Fig. 11. *F*-weighted optimal 4th order NTF (Dunn, Sandler, 1995).

6. Improved psychoacoustic noise shaping

The *F*-weighting curve introduced in Subsec. 5.3 represents a diffuse-field cor-
rected variant of the 15-phon equal-loudness contour specified in the ISO standard
226 (International Org. for Standardization [ISO], 2003). Adopting such a con-
tour as $W(f)$ in a noise shaping system supposedly renders the truncation noise
perceptually uniform at loudness levels of 15-phon and as stated by Helmrich
and his colleagues in their studies (Helmrich *et al.*, 2007), does not guaran-
tee minimal audibility of the truncation noise. This statement was based on an
investigation of the equal-loudness contours in (ISO, 2003), which reveals two
major issues with audio data truncation. The first issue can be identified by the
scope of the standard 226, revision 2003 (ISO, 2003), which "specifies combina-
tions of sound pressure levels and frequencies of pure continuous tones, which
are perceived as equally loud by human listeners". Helmrich and his colleagues
(Helmrich *et al.*, 2007) suggested that the noise spectrum produced by dithered
truncator shouldn't be regarded as a combination of pure tones. This view was
supported by (Stuart, 1994, cited by Stuart, 1997, cited by The Wikimedia
Foundation Inc., 2007) where it is suggested that the inner ear acts like a bank
of narrow-band filters. The bandwidth of each filter is proportional to its center
frequency, so as the frequency increases, a wider portion (in absolute terms) of

spectral energy is "collected" from a noise source. Accordingly, sensitivity to noise differs markedly from sensitivity to pure tones. The second issue that should be considered when selecting a perceptual weighting function for noise shaping is the potential discrepancy between listening conditions. The equal-loudness contours specified in the ISO standard 226 (which was the basis for the F-weighting curve) were measured in a non-reflective environment (freefield conditions) in which the sound source is directly in front of the listener. In fact, listening conditions in a real world (diffuse-field equalized headphones and two or more loudspeakers in a more or less reflective room) differ considerably from a freefield environment for which the contours in (ISO, 2003) apply. Given the two issues outlined above, Helmrich and his colleagues (HELMRICH et al., 2007) used the ITU-R 468-4 (International Telecomm. Union, Radiocommunication Assembly, 1986) noise weighting curve as a basis for truncation noise shaping optimization. The ITU-R 468-4 defines a weighting network based on data from experiments performed by British Broadcasting Corporation (BBC) and it was a response to calls for a weighting curve providing satisfactory agreement with subjective evaluations. Its spectrum (shown inverted in Fig. 12) peaks at 6.3 kHz, whereas the F-weighting contour exhibit maximum gain around 3.5 kHz. Helmrich and his colleagues modified ITU-R 468-4 curve (HELMRICH et al., 2007) – it's identical to original ITU-R 468-4 for frequencies from 1 to 12 kHz, but above 12 kHz, they customized it by modeling a steeper progression for high frequencies by applying cubic spline extrapolation. The motive behind this modification is the observation that the ear's sensitivity to high frequencies rapidly declines above approximately 12 kHz (ZWICKER, FASTL, 1990, cited by LIPSHITZ et al., 1991, cited by ZÖLZER, 1997).
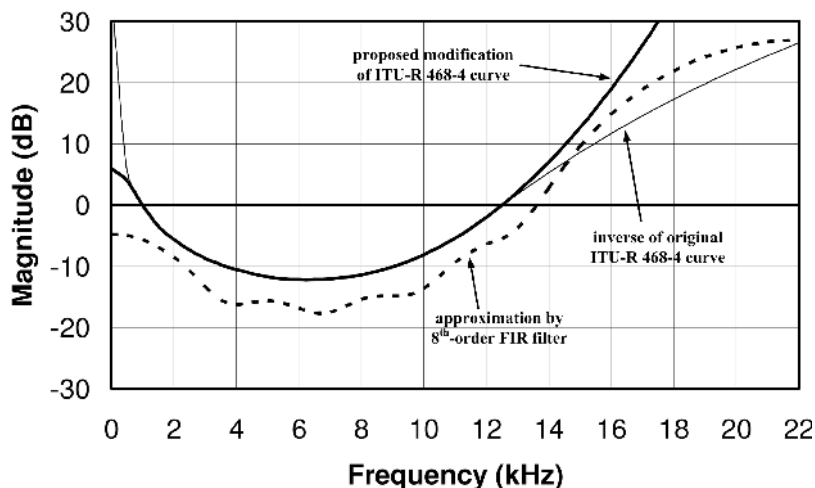

Fig. 12. Proposed modification of ITU-R 468-4 weighting curve (HELMRICH et al., 2007).

Besides the frequency-dependent loudness of noise (considered above), Helmrich and his colleagues (HELMRICH et al., 2007) examined two other psychoa-

coustic effects in the design of noise-shaping truncators: simultaneous and temporal masking. Simultaneous masking occurs when a signal becomes inaudible in the presence of a masker and, on the other hand, temporal masking of a signal takes place before (pre-masking) and after (post-masking) the presentation of the masker and is only of relatively short duration (ZWICKER, FASTL, 1990). If the input to a noise-shaping truncator is seen as the masker signal, simultaneous masking can be exploited as a means to minimize the relative audibility of the truncation noise. The effect of simultaneous masking (and to some extent, of temporal masking) depends greatly on the spectral content of both masker and masked signal (ZWICKER, FASTL, 1990). This implies that the noise shaping spectrum should resemble the input spectrum in order to achieve minimal audibility. The frequency content of typical signals such as music or speech, however, varies over time, so the noise shaping spectrum must be updated regularly, which leads to time-variant noise shapers (Fig. 13). As a basis for optimization, Helmrich and his colleagues in (HELMRICH *et al.*, 2007) used time-variant noise shaper based on Least Squares approach presented in (VERHELST, KONING, 2002). There, the following simplified psychoacoustic model is applied to obtain $W(f)$:

$$W\left(f_k = \frac{2\pi k}{N}\right) = \frac{1}{\beta P_{XX}(f_k) + (1 - \beta)P_{TQ}(f_k)}, \tag{28}$$

where $P_{XX}(f_k)$ represents the power spectrum of a 512-point Hanning-windowed segment of input signal $x(n)$. $P_{TQ}(f_k)$, the threshold in quiet, denotes the spectrum of the 9th-order filter approximating the inverse F-weighting curve. The scaling factor β epends on the window size ($N = 512$ is used) and the wordlength (in bits) of the input $x(n)$. $W(f_k)$ is updated every 256 input samples. While this adaptive psychoacoustic approach was found to weaken the truncation noise during signal portions of moderate and high level (VERHELST, KONING, 2002), HELMRICH and his colleagues (HELMRICH *et al.*, 2007) observed that a significant amount of noise shaping potential is left unused. In relatively loud segments, the unweighted truncation noise power tends to decline considerably
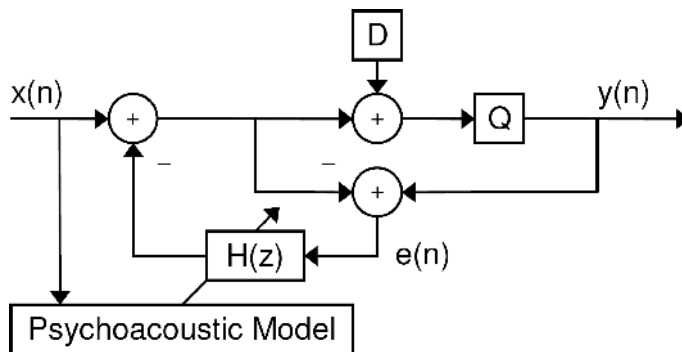

Fig. 13. Time-variant DSDM model with adaptive feedback filter H(z) controlled by a psychoacoustic model (HELMRICH *et al.*, 2007).

– the louder and more spectrally complex a signal part is, the lower the truncation noise power tends to be for this part. The reason for this phenomenon is the strong adaptation of the noise shaping filter to high-level signals. In typical signals such as music or speech, most of the spectral energy is contained in the lower frequencies up to about 10 kHz (ZWICKER, FASTL, 1990). High levels in this region, therefore, cause the truncation noise to rise above the absolute threshold in quiet, as approximated by $P_{TQ}(f_k)$. Consequently, the noise shaping spectrum produced by the filter determined with $W(f_k)$ from Eq. (28) shows a decrease in a high-frequency gain relative to its logarithmic average. In other words, the noise spectrum tends to "flatten" (HELMRICH et al., 2007). From this observation, HELMRICH and his colleagues (HELMRICH et al., 2007) concluded that the truncation noise produced by an adaptive noise shaper can be kept at a relatively high level for the range from approximately 15 kHz up to $f_s/2$ and that an overall reduction in noise loudness can be expected as more noise energy is shifted to the less audible upper end of the spectrum. Helmrich and his colleagues (HELMRICH et al., 2007) achieved constant truncation noise power by fixation of the high-frequency filter response by "stretching" the amplitude spectrum of $P_{TQ}(f_k)$ based on the spectral content of $P_{XX}(f_k)$. For this purpose, the portion of the spectral power in $P_{XX}(f_k)$ lying above the threshold defined by $P_{TQ}(f_k)$ was determined by:

$$S_k = \sum_{k=0}^{N/2-1} (\log_{10} d(k),\, d(k) > 1), \qquad N = 512, \tag{29}$$

where

$$d(k) = \frac{P_{XX}(f_k)}{P_{TQ}(f_k)} \tag{30}$$

$P_{TQ}(f_k)$ was then expanded in magnitude range to yield the fundamental spectrum for the instantaneous masking threshold (HELMRICH et al., 2007):

$$P'_{TQ}(f_k) = P_{TQ}(f_k)^{1+(S_k/S_{\max})}, \qquad S_{\max} = 2.7\frac{N}{2}. \tag{31}$$

Finally, $P_{TQ}(f_k)$ was replaced with $P'_{TQ}(f_k)$ in Eq. (28) to attain $W(f_k)$, that is, the inverse of the desired improved filter spectrum.

6.1. Listening experiments

Helmrich and his colleagues (HELMRICH et al., 2007) performed two listening tests with different types of transducers. Tests were prepared and executed according to MUSHRA (Multi-Stimulus test with Hidden Reference and Anchor) methodology (International Telecomm. Union, Radiocomm. Assembly, 2003, cited by VINCENT, 2005) with the following changes (in order to decrease the variance of the results):

- instead of the 3.5-kHz low-pass filtered anchor stimulus, a dithered truncated signal with a flat error spectrum was chosen (HELMRICH *et al.*, 2007),
- test subjects were asked to assign a grade of zero to the stimulus which they judged as having the lowest overall quality. The recommended instructions (International Telecomm. Union, Radiocomm. Assembly, 2003) do not require this explicitly (HELMRICH *et al.*, 2007).

Figure 14 illustrates the results of two listening experiments. For each noise shaper under test, the arithmetic average of the individual assessments (the mean opinion score, MOS) was given. A significance level of 95% was used to determine the confidence interval for each MOS (HELMRICH *et al.*, 2007). While the *F*-weighting noise shaper yields a significant perceptual improvement over plain truncation without noise shaping, it is clearly outperformed by modified ITU-R 468-4 filter design presented in Sec. 6. In the headphone test, truncation without noise shaping was scored lowest by all subjects. The *F*-weighting filter achieved satisfactory results, but its overall quality was rated lower than modified ITU-R 468-4 filter design. The adaptive noise shaper design was judged superior to all other implementations by most subjects. Nonetheless, a clear advantage over the static filter design was only observed at moderate and high signal levels. As reported by most subjects, low-level noise similar to that in other stimuli became audible during quiet signal passages (HELMRICH *et al.*, 2007).
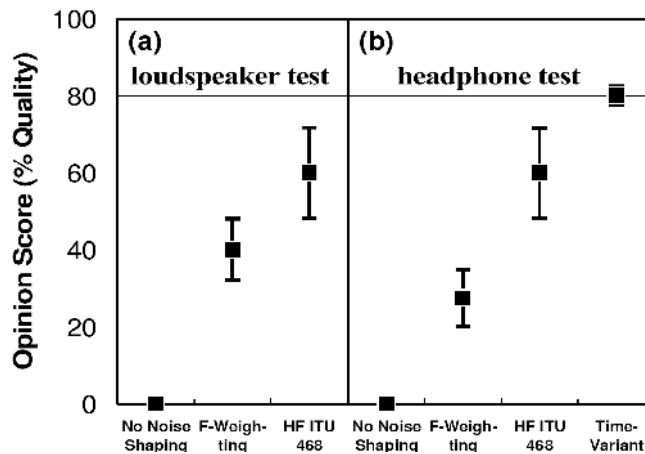

Fig. 14. Results of the two listening experiments (HELMRICH *et al.*, 2007).

7. Conclusion

In the last few years a large number of works focusing on the optimization of the NTF have been written. Based on extensive simulations, experiments and complex analysis, some kind of "guides" for the NTF designing and optimization were established. After designing the optimum noise transfer function, its coeffi-

cients should be matched to the specific structure of the sigma-delta modulator. Chosen methods for realizing NTF in a specific structure are shown in (Kuo *et al.*, 1999; Schreier, Temes, 2005; Yetik *et al.*, 2007; Ho *et al.*, 2009). In addition, software solutions for designing sigma-delta modulators from scratch are available. One of the most popular is Schreier's *Delta Sigma Toolbox* (Schreier, Temes, 2005). When designing audio DACs, it is worth examining closely the NTF optimization procedure based on the psychoacoustically optimal truncation noise shaping, as described in Subsec. 5.3 and Sec. 6. The approach and results of the paper will be used by the author of this paper for further optimization of the digital sigma-delta audio DAC in order to make the truncation noise invariant with changes of the input signal and make it less audible. In addition, investigation performed in (Kostrzewa *et al.*, 2003) shown that a group delay fluctuations in sigma-delta modulators exist with amplitude correlated with a period of stimulated signal and inversely proportional to its slew rate. This may affect the character of a sound and it appears advisable to perform further investigations on a time performance of sigma-delta modulators with e.g. *Time-Frequency Toolbox* (Auger *et al.*, 1996).

References

1. Anastassiou D. (1989), *Error Diffusion Coding for A/D Conversion*, IEEE Trans, on Circuits and Systems, **36**, 9, 1175–1186.

2. Auger F., Flandrin P., Gonçalvès P., Lemoine O. (1996), *Time – Frequency Toolbox*, Reference Guide, http://tftb.nongnu.org/refguide.pdf.

3. Bourdopoulos G.I. (1999), $\Sigma\Delta$ *modulators, Modeling, Design, Implementation, Applications*, Ph.D. Thesis (in Greek), Patras, Greece.

4. Bourdopoulos G.I, Pneumatikakis A., Anastassopoulos V., Deliyannis T.L. (2002), *Optimal NTFs for single bit $\Sigma\Delta$ Modulators*, DSP 2002, 14th International Conference on Digital Signal Processing, **2**, pp. 877–880, July 1–3, Sandorini.

5. Bourdopoulos G.I, Pneumatikakis A., Anastassopoulos V., Deliyannis T.L. (2003), *Delta-sigma modulators: modeling, design and applications*, Imperial College Press.

6. Chao K.C.H., Nadeem S., Lee W.L., Sodini C.G. (1990), *A Higher Order Topology for Interpolative Modulators for Oversampling A/D Converters*, IEEE Trans. on Circuits and Systems, **37**, 3, 309–318.

7. Dunn C. (1994), *Psychoacoustic Modeling of Nonlinear Errors*, in Measurement of Nonlinear Errors in Audio Electronics, Ph.D Thesis, University of Essex, UK.

8. Dunn C., Sandler M. (1995), *Psychoacoustically Optimal Sigma-Delta Modulation, Signals, Circuits and System Group*, Department of Electronic and Electrical Engineering, King's College, London WC2R 2LS, UK, 99th Convention of the Audio Engineering Society, New York.

9. Helmrich C.R., Holters M., Zölzer U. (2007), *Improved Psychoacoustic Noise Shaping for Requantization of High-Resolution Digital Audio*, AES 31st International Conference, London, UK.

10. Ho Y.H.K., Kwan H.K., Wong N., Ho K.L. (2009), *Designing globally optimal delta-sigma modulator topologies via signomial programming*, International Journal of Circuit Theory and Applications, **37**, 453–472.

11. International Telecomm. Union, Radiocommunication Assembly (1986), *Recommendation ITU-R BS. 468-4: Measurement of Audio-Frequency Noise Voltage Level in Sound Broadcasting.*

12. International Org. For Standardization (2003), *ISO 226:2003: Acoustics – Normal Equal-Loudness – Level Contours*, Geneva, Switzerland.

13. International Telecomm. Union, Radiocommunication Assembly (2003), *Recommendation ITU-R BS.1534-1: Method for the Subjective Assessment of Intermediate Quality Level of Coding Systems.*

14. Kostrzewa M., Kulka Z., Nykiel P. (2003), *Badanie wlasciwosci czasowych modulatorów delta-sigma*, Prace Naukowe Instytutu Telekomunikacji i Akustyki Politechniki Wroclawskiej, nr 84, Seria: Konferencje nr 28, Wrocław, 103–108.

15. Kulka Z. (2006), *Analog-to-Digital and Digital-to-Analog Converters for High-Quality Musical Sound*, Proc. of the XIth Symposium AES – New Trends in Audio and Video, Białystok, Proc. No. 134, Vol. 1.

16. Kulka Z., Woszczek P. (2008), *Implementation of digital sigma-delta modulators for high-resolution audio digital-to-analog converters based on field programmable gate array*, Archives of Acoustics, **33**, 1, 93–101.

17. Kulka Z., Lewandowski M. (2009), *An FPGA-based sigma-delta audio DAC*, Elektronika, 4, 107–111.

18. Kuo T.H., Chen K.D., Chen J.R. (1999), *Automatic coefficients design for high-order sigma-delta modulators*, IEEE Trans. Circuits Syst. II, Analog. Digit. Signal Process., **6**, 1, 6–15.

19. Lipshitz S., Vanderkooy J., Wannamaker R.A. (1991), *Minimally Audible Noise Shaping*, J. Audio Eng. Soc., **39**, 836–852.

20. Løkken I. (2005), *High-Resolution Audio DACs*, Final Report, A Review of the Digital Audio Conversion Process.

21. Norsworthy S.R., Schreier R., Temes G.C. (1997), *Delta-Sigma Data Converters, Theory, Design and Simulation*, IEEE Press, New York.

22. Schreier R. (1993), *An Empirical Study of High-Order Single-Bit Delta-Sigma Modulators*, IEEE Trans, on Circuits and Systems-IT. Analog and Digital Signal Processing, **40**, 8, 461–466.

23. Schreier R., Temes G.C. (2005), *Understanding Delta-Sigma Data Converters*, IEEE Press, Wiley Interscience, New York.

24. Stuart J.R. (1994), *Noise: Methods for Estimating Detectability and Threshold*, J. Audio Eng. Soc., **42**, 3, 124–140.

25. Stuart J.R. (1997), *Coding High Quality Digital Audio*, Meridian Audio Ltd., UK, www.meridian-audio.com/ara/coding2.pdf.

26. Verhelst W., Koning De D. (2002), *Least Squares Theory and Design of Optimal Noise Shaping Filters*, AES 22nd International Conference, Espoo, Finland.

27. VINCENT E. (2005), *MUSHRAM: A Matlab interface for MUSHRA listening tests*, User Guide, www.elec.qmul.ac.uk/people/emmanuelv/mushram.

28. WANNAMAKER R.A. (1992), *Psychoacoustically Optimal Noise Shaping*, J. Audio Eng. Soc., **40**, 611–620.

29. The Wikimedia Foundation Inc. (2007), *Equal-Loudness contour*, Wikipedia, the free encyclopedia, http://en.wikipedia.org/wiki/Equal-loudness_contour.

30. YETIK É., SAGLAMDEMIR O., TALAY S., DÜNDAR G. (2007), *A Coefficient Optimization and Architecture Selection Tool for $\Sigma\Delta$ Modulators in MATLAB*, Proceedings of the 17th ACM Great Lakes symposium on VLSI, 423–428.

31. ZÖLZER U. (1997), *Digital Signal Processing*, 3rd printing, Wiley, Chichester, England.

32. ZWICKER E., FASTL H. (1990), *Psychoacoustics: Facts and Models*, 2nd edition, Springer-Verlag, Berlin, Germany.